Available online at www.sciencedirect.com
ScienceDirect
International Journal of Mass Spectrometry 258 (2006) 113–119
International Journal of Mass Spectrometry
www.elsevier.com/locate/ijms

Aerosol MALDI of peptides and proteins in an ion trap mass spectrometer: Trapping, resolution and signal-to-noise

William A. Harris, Peter T.A. Reilly *, William B. Whitten

Oak Ridge National Laboratory, PO Box 2008, MS 6142, Oak Ridge, TN 37831, United States

Received 5 May 2006; received in revised form 19 June 2006; accepted 21 June 2006
Available online 18 July 2006

Abstract

The aerosol MALDI technique has been noted for its extreme sensitivity. Unfortunately, resolution and signal quality remain as issues that limit the applicability of the technique. Utilizing the aerosol MALDI technique in an ion trap mass spectrometer has an advantage because the resolution and signal-to-noise ratio are not products of the laser ablation event. In this study, the mass dependence of the aerosol MALDI technique in a constant frequency, 1 MHz, ion trap was explored in terms of trapping, resolution and signal-to-noise. Mass resolution exceeding 5000 was achieved for substance P. Trapping and detection of ions up to myoglobin, *m/z* 16.9 kDa, was demonstrated. The effect of the pseudo-potential well depth at ejection on resolution and signal-to-noise was revealed. Our results show that the ability to trap large ions with the aerosol MALDI technique can be modeled with the MALDI-induced velocity distribution and the trapping pseudo-potential well depth.

Keywords: Aerosol; MALDI; Ion trap; Real time

1. Introduction

There are many sources of bioaerosols. It has long been a goal of aerosol scientists to be able to differentiate, speciate and count airborne bioparticles in real time. The benefits of achieving this goal are numerous. Aside from the ability to monitor the air for bioterror weapons, there is also the need to be able to accurately define how diseases are transmitted, the need to track and identify other airborne pathogens such as those that cause sick building syndrome and a variety of other health related issues such as allergens. Unfortunately, bioaerosols have a wide variety of chemical and physical properties that make this task very difficult.

Much of the initial work in single-particle mass spectrometry of bioaerosols focused on bacteria [1–5]. While identifiable mass spectral fingerprints were observed, attempts to identify, speciate, and count individual airborne bacteria were mixed [1–5]. Due to charge-transfer effects during the desorption and ionization process, the final ion distribution is defined by the relative ionization potentials and electron affinities of the species in the particle matrix [6]. For bacteria, the majority of mass spectral intensity was below 200 Da [2,4,5] and was attributed to alkali metal adducts and phosphates by tandem mass spectrometry [2]. Because the nature of the material that could be associated with airborne bacteria particles is unknown, the use of direct laser desorption aerosol mass spectrometry for identifying and counting airborne bacteria remains dubious.

Perhaps the best chance of directly identifying and counting individual bioaerosol particles is by mass spectrometric measurement of the high mass species, such as proteins [7,8] and phospholipids [9] that can make up a large part of the biological material of the particle. In order to accomplish this with aerosol mass spectrometry, the technique had to be modified to extend the range of masses analyzed. Fortunately this can be done by addition of a matrix that permits ionization of these large mass species. Murray et al. [10] were the first to incorporate aerosols into the MALDI process. Mansoori et al. [11] made improvements by making it a single-particle technique. Stowers et al. [12] further improved the technique by coating the particles on-the-fly before admission into their mass spectrometer. With their technique, they generated mass spectra of individual bacterial spores [12,13]. Other groups have also demonstrated MALDI on a single-particle level by either on-line coating of the particles [14,15] or premixing the matrix and analyte [16,17].

* Corresponding author. Tel.: +1 865 574 4919; fax: +1 865 574 8363.
E-mail address: reillypt@ornl.gov (P.T.A. Reilly).

1387-3806/$ – see front matter © 2006 Elsevier B.V. All rights reserved.
doi:10.1016/j.ijms.2006.06.014

Our group has extended single-particle MALDI for use with an ion trap mass spectrometer for bioaerosols with masses up to 1500 Da [18]. We illustrated the advantage of using tandem mass spectrometry to identify the biomolecules.

In this work, we demonstrate the applicability of the aerosol MALDI ion trap technique for the analysis of biomolecules in excess of 1500 Da. Aerosol MALDI mass spectra of known proteins were obtained as a function of increasing mass up to myoglobin (*m*/*z* 16,951) with a modified commercial ion trap (Polaris Q, ThermoFinnigan, Austin, TX). Our goal was to determine the factors that define the mass limits of the trap in terms of trapping and detecting biomolecular ions. We have investigated the factors that define the resolution and signal-to-noise ratio of the trap and suggested ways of improving the technique to obtain high resolution mass spectra in the high mass range in an ion trap.

2. Experimental methods

The experimental setup is shown in Fig. 1. Polydisperse biomolecule-containing particles were generated with a Collison nebulizer using deionized water as a solvent. The nebulized aerosol was passed through heated and cooled tubes consecutively to desorb the solvent from the particles and then condense it on the cooled wall to dry the aerosol. The emerging aerosol then entered the matrix applicator consisting of a heated saturator and condenser. The saturator was a 15 cm long, 19 mm diameter, heated glass tube. Ferulic acid crystals were deposited in the saturator and heated to 130 °C. This matrix was chosen because it works well with 355-nm excitation and yields high mass ions. Inside the heated saturator, the aerosol and matrix vapor were in equilibrium so that the rate of deposition was equal to the rate of sublimation. Upon leaving the saturator, the aerosol and matrix vapor were cooled to 10 °C resulting in a supersaturation that causes the matrix vapor to rapidly condense onto the aerosol particles. The amount of matrix added to the surfaces of the particles was dependent on the linear flow rate and the saturator temperature. Up to a few 100 nm of matrix could be added to the radius of the particles [18]. The flow rate through the Collison nebulizer and matrix coating apparatus ranged between 0.5 and 1.5 L/min. The residence time in the saturator ranged from 5 to 1.7 s, respectively. Aerosol generation and coating were performed at atmospheric pressure. A diagram of the aerosol generator, matrix applicator, and mass spectrometer is shown in Fig. 1. This design is similar to that used by Stowers et al. [12] and in condensation nuclei counters in commercial particle sizing instruments.

A portion of the coated aerosols was drawn into the instrument and analyzed on an individual particle basis in real time with our ion trap-based aerosol mass spectrometer. The spectrometer used herein has been described in detail elsewhere [19]. It is an updated and transportable version of the instrument used previously in our laboratory [20]. Our present instrument was converted from a commercially available ion trap mass spectrometer (Polaris Q, ThermoFinnigan, Austin, TX). The commercial system was minimally modified by replacing the top blank flange with one that contained our inlet, light scattering detection optics and laser ablation optics. In addition, four holes were drilled into the ring electrode to pass the particle beam and the ablation laser. The GC inlet and ionization source have not been modified and the instrument can still operate as a detector for a gas chromatograph, its original purpose.

With these modifications, the instrument now operates as an aerosol mass spectrometer. First, an aerodynamic lens-based inlet system, based on the design of Liu et al. [21,22] produced an extremely well-collimated particle beam from an aerosol admitted in to the instrument through a 100-μm diameter orifice. A series of constrictions and expansions forced the particles toward the central axis of the lens system. The trajectory lines of the par-

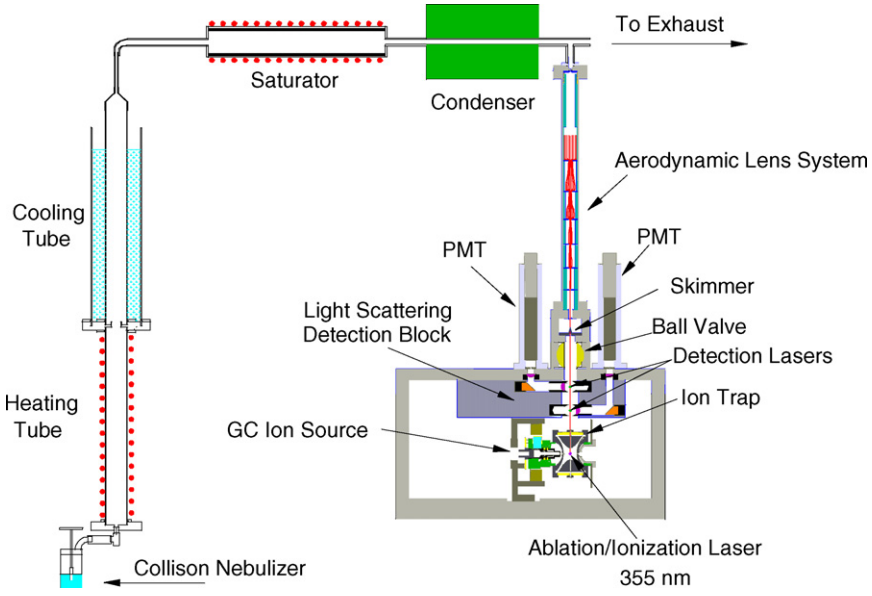

Fig. 1. Schematic diagram of the instrument showing the bioaerosol generation, matrix coating and the ion trap-based individual particle aerosol MALDI mass spectrometer.

ticles in the lens system have been represented in Fig. 1. Because the particles were moving along the central axis during the final expansion into vacuum, they experienced minimal radial dispersive force and remained collimated. The particle beam was further separated from the atmospheric carrier gas by passage through a 250-μm diameter skimmer into the main chamber of the ion trap mass spectrometer.

Inside the main chamber, the collimated particle beam passed through two focused 532-nm diode laser beams propagating into and out of the page in Fig. 1. The scattered light from each laser was collected and focused onto separate photomultiplier tubes (PMT) through a pinhole to minimize background scattered light. The PMT signals were inverted and converted to TTL pulses that were used to measure the time-of-flight between the two detection points. The measured flight time provided a direct correlation that determined the aerodynamic size of each measured particle. In this work, measured aerodynamic particle sizes range from 500 to 1000 nm. The scattered light signals also permit the timing of a focused 355-nm ablation/ionization laser to fire when the particle arrives at the center of the ion trap regardless of its size or velocity. The timing circuit is also designed to produce a TTL pulse to fire the flashlamps of the YAG laser at the optimal time (150 μs) before the detected particle reaches the center of the ion trap. Because the minimum flight time between the second detection point and the center of the ion trap is greater than the optimal 150 μs delay, there are no limitations to the size of the particles that may be analyzed other than the ability to detect the scattered light from the 532-nm detection lasers. The nascent ions created by the 355-nm laser pulse were trapped and subsequently subjected to standard mass analysis techniques [19]. Ions were detected with the channeltron detector. Under normal operating conditions, a high mass limit of 1000 *m/z* was obtained. This mass range was extended through high mass resonance ion ejection [23] via user-based custom interface software based on the Xcalibur Development Kit (ThermoFinnigan). For these experiments, the ring electrode of the ion trap was usually held at an rf voltage where low mass ions are immediately ejected, thus improving sensitivity for high masses. The scan rate depends on the scan function required. Generally, our scan time was 450 ms with 33 data points measured per ms. Typically 600 ms was required from particle detection to data storage.

3. Results and discussion

Peptide-containing bioaerosols were coated in the matrix applicator with ferulic acid. A portion of the coated aerosol was then directed into the instrument where the individual particles were sized, ablated, and mass analyzed. Intense signals were recorded for peptides on a single-particle basis. An example of this is shown in Fig. 2a for a 625-nm particle containing approximately 20 amol of substance P. The parent ion isotopes were resolved with a peak width (FWHM) of 0.25 Da, resulting in a resolution over 5300. The substance P mass spectrum was recorded with an ejection q of 0.6 and a scan rate of 0.450 ms/amu. Strong signals were recorded for single-particles of insulin chain B as shown in Fig. 2b for a 950-nm particle

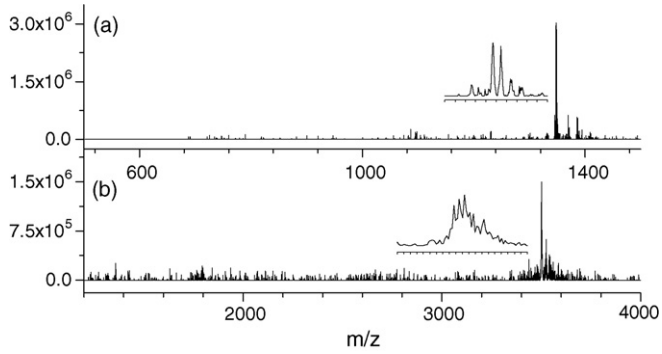

Fig. 2. Single-particle MALDI mass spectra from (a) a 625 nm particle of substance P (*m/z* 1348.7); (b) a 950 nm particle of insulin chain B (*m/z* 3496.9).

containing approximately 50 amol. The insulin chain B mass spectrum was acquired with an ejection q of 0.225 with a scan rate of 0.110 ms/amu. Although not completely resolved, some isotopic structure is observed, even with a scan rate four times than that utilized in the substance P mass spectrum in Fig. 2a.

Application of the matrix was limited so that particles were not observed without input of analyte particles into the saturator. In this limit, analyte ion intensity did not seem to change much on average. Typically at least a 150–nm thick coating of matrix was required to yield consistent signal. A more detailed study of the effect of matrix thickness on analyte signal deserves further study. The percentage of laser pulses that yielded a useful mass spectrum for peptides was roughly the same as polybeads of a similar size; however, that percentage decreased with increasing analyte mass.

Mass resolution was not affected by averaging. To demonstrate this, 100 spectra of substance P were averaged and are displayed in Fig. 3A. The inset shows a close-up look at the averaged substance P parent ions. Baseline resolution was observed and a resolution of 5000 (measured at FWHM) was calculated for the parent ions. This observed resolution is approximately an order of magnitude greater than that reported for time-of-flight-based aerosol MALDI [12,16,17,24]. In those instruments, aerosol beam width and methods of sample preparation have been suggested as limiting resolutions [13]. In addition, lower resolution linear flight tubes are preferred over reflectrons due to ion loss in the latter [13,24]. In contrast, our technique traps the MALDI ions after creation and subsequently collisionally cools them before mass analysis in the ion trap thereby decoupling the MALDI process from the mass analysis. This is the reason that very high resolution has been obtained from MALDI generated ions on ion traps and q-TOFs [25,26]. Our technique minimizes the implications of aerosol beam width, ion initial velocities, and the sample preparation method on the mass analysis. Thus in our case, the resolution is a function of instrumental mass scan parameters, not the laser ablation event.

In Fig. 3, a progression of averaged aerosol MALDI spectra as a function of increasing analyte mass is presented: (A) substance P (*m/z* 1348.7, ejection $q = 0.6$); (B) melittin (*m/z* 2847.5, $q = 0.3$); (C) insulin chain B (*m/z* 3496.9, $q = 0.225$); (D) insulin (*m/z* 5734.6, $q = 0.15$); (E) ubiquitin (*m/z* 8565.6, $q = 0.09$); (F) cytochrome *c* (*m/z* 12232.0, $q = 0.06$); (G) myo-

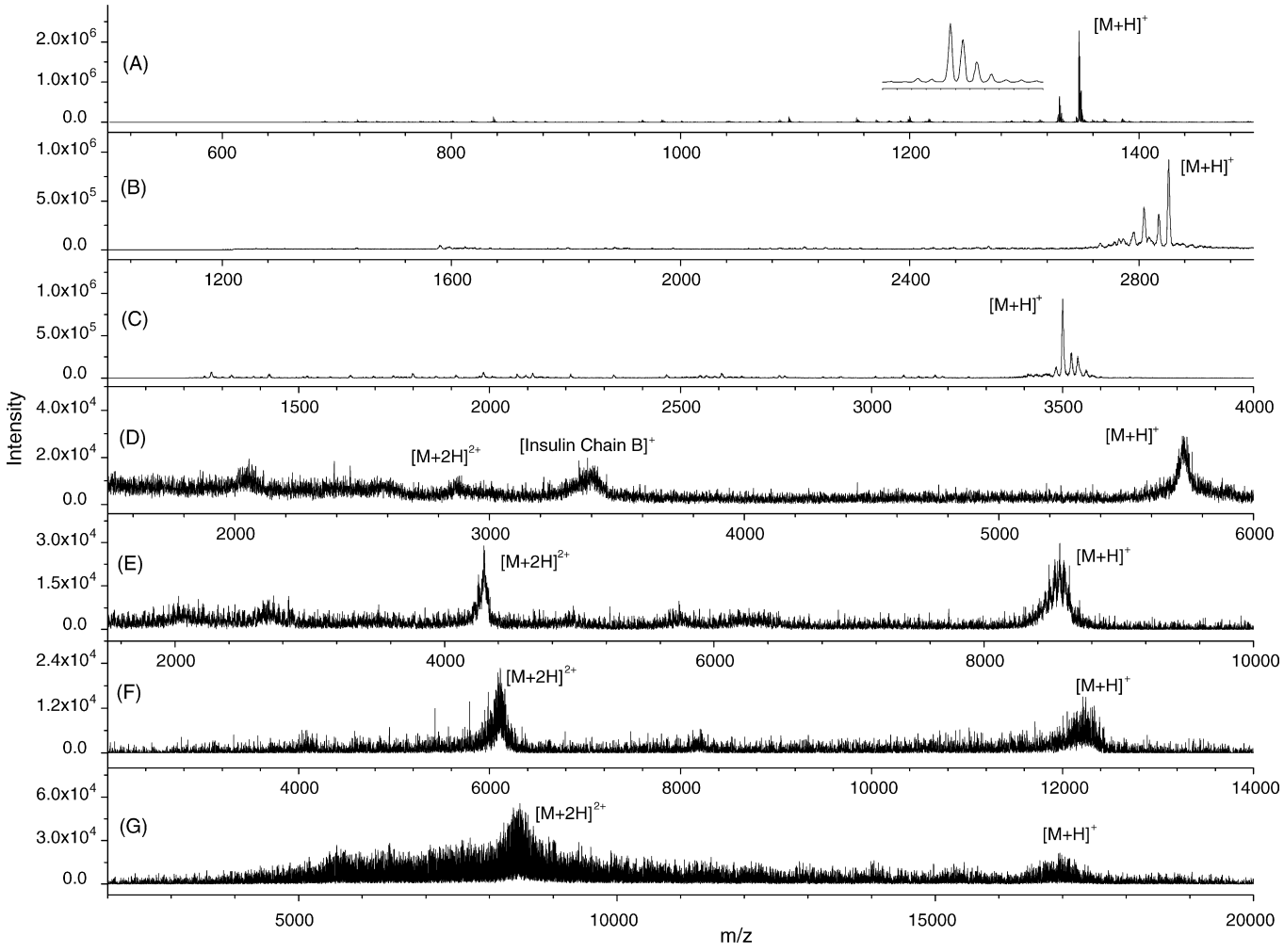

Fig. 3. Averaged aerosol MALDI mass spectra from 100 individual particles of (A) substance P (*m/z* 1348.7); (B) melittin (*m/z* 2847.5); (C) insulin chain B (*m/z* 3496.9); (D) insulin (*m/z* 5734.6); (E) ubiquitin (*m/z* 8565.8); (F) cytochrome *c* (*m/z* 12232.0); (G) myoglobin (*m/z* 16952.5).

globin (*m/z* 16952.5, $q = 0.045$). Examination of the series of spectra in Fig. 3 shows a steady decline in analyte ion intensity from approximately 3 million (arbitrary units) for substance P (*m/z* 1348.7) to less than 20,000 for myoglobin (*m/z* 16952.5). Because the size distributions of the particles in each of the spectra were roughly the same, there was only an order of magnitude change in the number of biomolecules available for ionization in the particles moving from substance P to myoglobin while maintaining equivalent analyte mass. This represents a factor of 150 change in signal intensity with only a factor of 10 change in the concentration on a mole basis. This suggests either that there is a reduction in ionization efficiency of the large *m/z* ions or they are not being trapped.

Examination of the distribution of doubly and singly charged analyte ions is insightful. Our series of spectra as a function of increasing analyte mass shows that the intensity of the doubly charged peak progressively overtakes the singly charged peak as a function of increasing analyte mass. The doubly charged species appeared with insulin (*m/z* 5734.6) and became about one-half the integrated intensity of the singly charged peak with ubiquitin (*m/z* 8565.8). The doubly and singly charged peak intensities were roughly equal for cytochrome *c* (*m/z* 12232.0) while the doubly charged peak of myoglobin (*m/z* 16952.5) eclipsed the singly charged mass peak. The MALDI process primarily yields singly charged species. The degree of multiple charging increases as a function of analyte mass and often depends on the sample preparation technique. However, MALDI TOF mass spectra of ions in the 17 kDa mass range in the literature have demonstrated that the ratio of doubly charged to singly charged species coming out of the matrix should not greatly exceed one, regardless of the preparation technique [13,27,28]. Moreover, the MALDI technique always produces a significant quantity of singly charged species even when looking at large analytes such as bovine serum albumin (66 kDa). Therefore, we suggest that the loss of intensity as a function of increasing mass was due to an inability to trap the more energetic higher mass species coming out of the MALDI process, not so much an inability to ionize the analyte.

The trapping limitations of the ion trap-based aerosol MALDI technique may be defined by the spatial kinetic energy distribution of the ablated species and the pseudo-potential well depth. In general, since the ions are created at the center of the ion trap,

if the ion kinetic energy is greater than the pseudo-potential well depth, it escapes. If it is less, the ion is trapped. Initial velocities distributions of MALDI generated ions from surfaces have been well studied and are independent of mass. Beavis and Chait [29] measured the average velocity from the MALDI process at 750 m/s with the extremes of the distributions extrapolated to roughly 300 and 1200 m/s. The position of the average and the width of the distribution are somewhat laser intensity dependent with the position of the average increasing and the width of the distribution narrowing with increasing laser intensity. Velocity distributions of ions from incomplete vaporization of individual particles have been measured and found to have a similar distribution to that seen from MALDI from a surface [30]. It is reasonable to suggest that the range of velocities created by MALDI from a surface are generalizable to the ablation plume created by MALDI from a single particle.

The spatial distribution of the ablation plume is particle size dependent. In the limit where the circumference of the particle is greater than the wavelength of the ablation laser, the majority of the ablation plume propagates in the direction of the laser [18]. In the limit where the particle circumference is less than the laser wavelength the ablation process is isotropic. This phenomenon has ramifications in an ion trap because the pseudo-potential well in the radial direction is one-half that in the direction of the end-cap electrodes [31]. This means that trapping efficiencies will be better for larger particles if the laser propagates in the direction of the end-cap electrodes. For small particles that are completely vaporized, trapping efficiencies will be independent of laser propagation.

For an ion trap of fixed frequency, the optimum condition for trapping the highest masses is to set the rf to its maximum voltage. Our instrument's maximum rf voltage is approximately 7500 $V_{0\text{–p}}$. The pseudo-potential well depth in the r and z directions are defined for $q_{r \text{ or } z} < 0.4$ as

$$D_r = \frac{q_r V_{0\text{–p}}}{8} \quad \text{and} \quad D_z = \frac{q_z V_{0\text{–p}}}{8}$$

And the radial and axial Mathieu parameters q_r and q_z, respectively, are given by

$$q_r = \frac{4eV}{[m(r_0^2 + 2z_0^2)\Omega^2]} \quad \text{and} \quad q_z = \frac{8eV}{[m(r_0^2 + 2z_0^2)\Omega^2]}$$

where e is the electronic charge, V the rf voltage (0–p), m the ion mass, r_0 the ring electrode radius, z_0 the distance between the center of the trap and the end-cap electrode and Ω is the radial frequency of the trapping potential given by 2π times the trap frequency. The frequency of our instrument is 1.0247 MHz.

With this information, we have calculated the radial and axial pseudo-potential well depths as a function of m/z in Fig. 4. In this figure, we have also included the kinetic energy of the ions coming out the MALDI process as a function of molecular weight for an array of velocities spanning the velocity distribution of the ions from the MALDI process.

The interpretation of Fig. 4 is somewhat dependent on experimental setup of the ablation laser and the size of the aerosol particles. In our instrument, the laser passes through the center of the trap through holes drilled through the ring electrode and

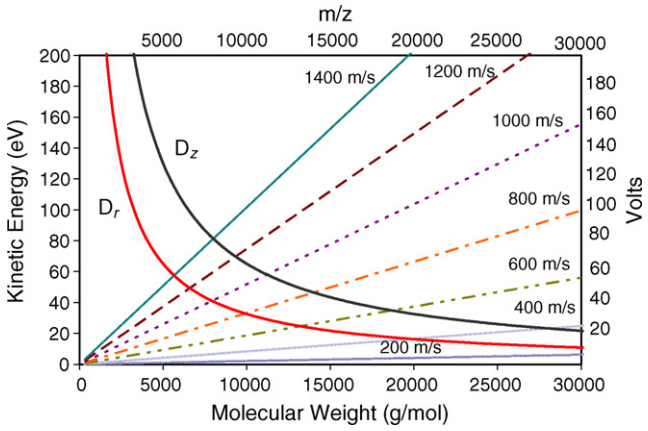

Fig. 4. Axial and radial pseudo-potential well depth D_z and D_r are presented as a function of mass to charge ratio, m/z and the MALDI expansion-induced kinetic energy as a function of molecular weight at incremental values of the velocity at 200, 400, 600, 800, 1000, 1200 and 1400 m/s.

the circumference of the matrix coated particles is greater than the wavelength of the laser. This means that the majority of the ablation plume travels in the radial direction. Consequently, the pseudo-potential well depth that best determines our ability to trap the MALDI ions created from individual particles ablated in the center of the trap is D_r.

If collision-induced damping is ignored, MALDI created ions travelling in the radial direction will escape the trapping potential if their kinetic energy is greater than eD_r. For any constant velocity line in the figure, masses to the left of the crossing with the radial well potential will be trapped. For example, the maximum velocity in the distribution of ions travelling in the radial direction is 1400 m/s then all ions below m/z 5560 will be trapped. If the average velocity in the radial direction is 750 m/s then only half of the ions will be trapped at roughly m/z 11,000. Accordingly, our ability to trap ions begins to decrease near m/z 6000 and therefore our sensitivity should begin to decline at that point as well. The limit of detection for our 1 MHz trap using the aerosol MALDI technique will be near m/z 20,000 because the population of ions falls dramatically in the vicinity of 400 m/s [29].

We believe this is evidence that we are producing significant amounts of singly charged myoglobin ions with our technique but cannot trap the majority of them because their MALDI-induced kinetic energy is too great to permit trapping. The velocity distribution of the MALDI process from a surface produces only a small fraction of the proteins with a velocity of 400 m/s or less [29]. If this is also true for the MALDI process from a single particle then only a tiny fraction of the myoglobin proteins will have low enough kinetic energy to be trapped by the radial pseudo-potential well. Therefore, we suggest that the place where the 400 m/s line crosses the radial pseudo-potential well curve in Fig. 4 is a reasonable prediction of the mass trapping limit for the aerosol MALDI process in a 1 MHz ion trap.

Two other trends in the mass spectra are presented in Fig. 5 as a function of increasing mass. These are reductions in the signal-to-noise ratio and resolution. Both of these trends have the same root cause. In order to extend the mass range of the

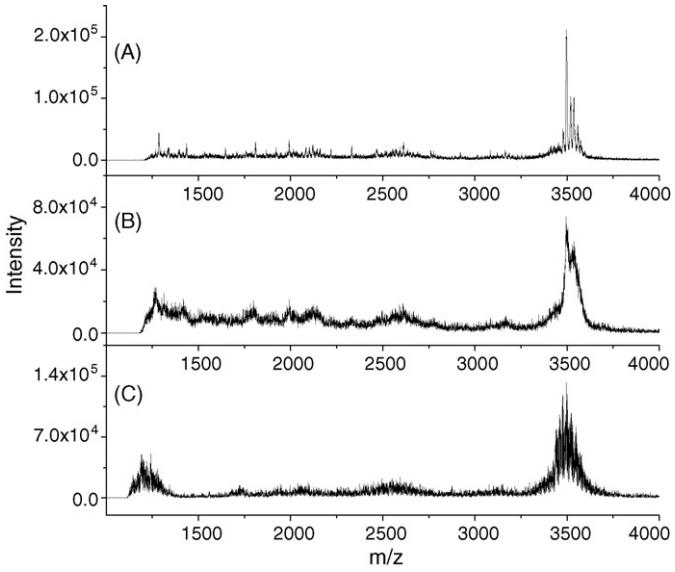

Fig. 5. Averaged aerosol MALDI mass spectra from 100 individual particles of insulin chain B as a function of decreasing q_z at ejection (A) $q_z = 0.23$ and $D_z = 189$ V; (B) $q_z = 0.15$ and $D_z = 120$ V; (C) $q_z = 0.06$ and $D_z = 50$ V.

instrument, we have used a technique developed by Cooks and coworkers [23] called resonant ejection. A supplemental potential is applied to the end-cap electrodes during the rf ramp. When the secular frequency of the ions matches the frequency of the applied supplemental potential during the ramp, the ions are ejected from the trap. The depth of the pseudo-potential well at the point of ejection is the major factor in defining the resolution and signal-to-noise ratio; the deeper the well, the better the resolution and signal-to-noise ratio [32,33]. Unfortunately, for an instrument with a fixed trapping potential frequency operating in the extended mass range, higher masses are ejected at lower values of q_z and D_z.

The effect of ejecting ions at lower values of q_z can be seen in Fig. 5A–C. Here we show the mass spectra of insulin chain B ejected at a q_z of 0.23, 0.15 and 0.06, respectively. These values of q_z at ejection correspond to pseudo-potential well depths of 189, 120 and 50 V. Goeringer et al. [32] derived an equation for resonant ejection mass resolution in an ion trap:

$$\frac{m}{\Delta m} = \frac{q_z \Omega}{2\sqrt{2}(\Delta\omega)}$$

where $\Delta\omega_0$ is the supplemental frequency line width that is proportional to the square root of the scan rate. When the trap frequency and scan rate are held constant increasing the Mathieu parameter q_z at ejection increases the resolution and the trap depth. The value of q_z at ejection can be increased while maintaining the rf voltage at ejection by increasing the frequency of the supplemental potential applied to the end-cap electrodes or decreasing the radial trapping frequency, Ω. This increases the pseudo-potential well depth at resonance ejection. Deeper potential wells at ejection increase resolution as shown in Fig. 5.

The noise level also increases with decreasing well depth. The observed noise is caused by the spontaneous escape of ions from the trap as evidenced by the reduction in the noise level at the right of Fig. 5 after the majority of ions have been ejected from the trap. Deeper potential wells at ejection make spontaneous escape of ions less probable and increase the signal-to-noise ratio. Consequently, deeper potential wells, higher resolution and higher signal-to-noise ratios are tied together.

From our aerosol MALDI spectra in Fig. 4, it becomes clear that the utility of the aerosol MALDI technique in a standard ion trap decreases for m/z greater than that for insulin chain B (m/z 3496.9) where the resolution begins to decline markedly. To increase the utility of the ion trap in the high mass range the frequency of the trapping potential should be decreased. This can be seen from the above equation for resolution by substituting the definition of q_z to get

$$\frac{m}{\Delta m} = \frac{eV2\sqrt{2}}{m(r_0^2 + 2z_0^2)\Omega(\Delta\omega)}$$

This equation demonstrates that it is feasible to maintain resolution at constant rf voltage and scan rate for higher masses by correspondingly reducing the trapping potential frequency, Ω. The proof of this concept was demonstrated by Ding et al. [34] with their digital ion trap. In this work, they swept the trapping frequency instead of the rf voltage when performing a mass scan, demonstrating a resolution for AP MALDI of myoglobin in excess of 2100 at a very rapid scan speed of 0.025 ms/amu [34]. Correspondingly slower scan speeds should produce better resolution. The combination of an ion trap with a reduced trapping potential frequency with aerosol MALDI should improve the trapping of higher mass ions, signal-to-noise and resolution. A digital ion trap with a reduced trapping potential frequency is currently under construction for use with aerosol MALDI.

4. Conclusions

Aerosol MALDI mass spectra of peptides with good signal-to-noise and resolution were obtained in a commercially available 1 MHz ion trap. Both single- and averaged-particle mass spectra were obtained with resolutions in excess of 5000, approximately an order of magnitude above that demonstrated with aerosol MALDI time-of-flight instruments. This suggests that instruments (ion traps, qTOFs, and ion trap-time-of-flight hybrids) that decouple the desorption and ionization process from the mass analysis step have performance advantages in aerosol MALDI. In our current configuration, performance degraded below an ejection q of 0.225 (mass limit of 4000 m/z). The limitations of the ion trap-based aerosol MALDI technique were explored in terms of mass, resolution and signal-to-noise. The ability of an ion trap to analyze large ions can be predicted by modeling the kinetic energy distribution of the ions from the MALDI process and comparing that to the pseudo-potential well depth by measuring and comparing the MALDI mass spectra as a function of analyte mass. 1 MHz traps are capable of trapping and detecting ions up to approximately 17 kDa with diminishing resolution and signal-to-noise. Trapping efficiency, resolution and signal-to-noise ratio were shown to diminish with decreasing pseudo-potential well depth. Finally, we suggested the feasibility of applying the technique in the higher mass range by reducing the trap frequency.

Acknowledgements

This research was funded by the Environmental Remediation Sciences Division, Office of Biological & Environmental Research, Environmental Management Science Program, U.S. Department of Energy, under contract No. DE-AC05-00OR22725 with Oak Ridge National Laboratory, managed and operated by UT-Battelle, LLC.

References

[1] M.P. Sinha, R.M. Platz, S.K. Friedlander, V.L. Vilker, Appl. Environ. Microbiol. 49 (1985) 1366.
[2] R.A. Gieray, P.T.A. Reilly, M. Yang, W.B. Whitten, J.M. Ramsey, J. Microbiol. Meth. 29 (1997) 191.
[3] E.P. Parker, M.W. Trahan, J.S. Wagner, S.E. Rosenthal, W.B. Whitten, R.A. Gieray, et al., Field Anal. Chem. Technol. 4 (2000) 31.
[4] A. Srivastava, M.E. Pitesky, P.T. Steele, H.J. Tobias, D.P. Fergenson, J.M. Horn, et al., Anal. Chem. 77 (2005) 3315.
[5] D.P. Fergenson, M.E. Pitesky, H.J. Tobias, P.T. Steele, G.A. Czerwieniec, S.C. Russell, et al., Anal. Chem. 76 (2004) 373.
[6] P.T.A. Reilly, A.C. Lazar, R.A. Gieray, W.B. Whitten, J.M. Ramsey, Aerosol Sci. Technol. 33 (2000) 135.
[7] A.J. Madonna, F. Basile, I. Ferrer, M.A. Meetani, J.C. Rees, K.J. Voorhees, Rapid Commun. Mass Spectrom. 14 (2000) 2220.
[8] C. Fenselau, P.A. Demirev, Mass Spectrom. Rev. 20 (2001) 157.
[9] Y. Ishida, A.J. Madonna, J.C. Rees, M.A. Meetani, K.J. Voorhees, Rapid Commun. Mass Spectrom. 16 (2002) 1877.
[10] K.K. Murray, T.M. Lewis, M.D. Beeson, D.H. Russell, Anal. Chem. 66 (1994) 1601.
[11] B.A. Mansoori, M.V. Johnston, A.S. Wexler, Anal. Chem. 68 (1996) 3595.
[12] M.A. Stowers, A.L. van Wuijckhuijse, J.C.M. Marijnissen, B. Scarlett, B.L.M. van Baar, C.E. Kientz, Rapid Commun. Mass Spectrom. 14 (2000) 829.
[13] A.L. van Wuijckhuijse, M.A. Stowers, W.A. Kleefsman, B.L.M. van Baar, C.E. Kientz, J.C.M. Marijnissen, J. Aerosol Sci. 36 (2005) 677.
[14] S.N. Jackson, S. Mishra, K.K. Murray, Rapid Commun. Mass Spectrom. 18 (2004) 2041.
[15] L. Zhou, Y. Zhu, X. Guo, W. Zhao, H.-Y. Zheng, X. Gu, et al., Sci. China: Ser. G Phys. Mech. Astronomy 49 (2006) 187.
[16] L. He, K.K. Murray, J. Mass Spectrom. 34 (1999) 909.
[17] S.C. Russell, G. Czerwieniec, C. Lebrilla, P. Steele, V. Riot, K. Coffee, et al., Anal. Chem. 77 (2005) 4734.
[18] W.A. Harris, P.T.A. Reilly, W.B. Whitten, Anal. Chem. 77 (2005) 4042.
[19] W.A. Harris, P.T.A. Reilly, W.B. Whitten, J.M. Ramsey, Rev. Sci. Instrum. 76 (2005).
[20] P.T.A. Reilly, R.A. Gieray, M. Yang, W.B. Whitten, J.M. Ramsey, Anal. Chem. 69 (1997) 36.
[21] P. Liu, P.J. Ziemann, D.B. Kittelson, P.H. McMurry, Aerosol Sci. Technol. 22 (1995) 293.
[22] P. Liu, P.J. Ziemann, D.B. Kittelson, P.H. McMurry, Aerosol Sci. Technol. 22 (1995) 314.
[23] R.E. Kaiser, R.G. Cooks, G.C. Stafford, J.E.P. Syka, P.H. Hemberger, Int. J. Mass Spectrom. Ion Process 106 (1991) 79.
[24] G.A. Czerwieniec, S.C. Russell, C.B. Lebrilla, K.R. Coffee, V. Riot, P.T. Steele, et al., J. Am. Soc. Mass Spectrom. 16 (2005) 1866.
[25] A.V. Loboda, A.N. Krutchinsky, M. Bromirski, W. Ens, K.G. Standing, Rapid Commun. Mass Spectrom. 14 (2000) 1047.
[26] J. Qin, R. Steenvoorden, B.T. Chait, Anal. Chem. 68 (1996) 1784.
[27] M. Karas, F. Hillenkamp, Anal. Chem. 60 (1988) 2299.
[28] M.D. Beeson, K.K. Murray, D.H. Russell, Anal. Chem. 67 (1995) 1981.
[29] R.C. Beavis, B.T. Chait, Chem. Phys. Lett. 181 (1991) 479.
[30] C.C. Vera, A. Trimborn, K.P. Hinz, B. Spengler, Rapid Commun. Mass Spectrom. 19 (2005) 133.
[31] R.E. March, R.J. Hughes, Quadrupole Storage Mass Spectrometry, John Wiley & Sons, New York, 1989.
[32] D.E. Goeringer, W.B. Whitten, J.M. Ramsey, S.A. McLuckey, G.L. Glish, Anal. Chem. 64 (1992) 1434.
[33] D.M. Chambers, D.E. Goeringer, S.A. McLuckey, G.L. Glish, Anal. Chem. 65 (1993) 14.
[34] L. Ding, M. Sudakov, F.L. Brancia, R. Giles, S. Kumashiro, J. Mass Spectrom. 39 (2004) 471.